Histology and Histopathology
From Cell Biology to Tissue Engineering

ORIGINAL ARTICLE   **Open Access**

Urolithin A attenuates bupivacaine-induced neurotoxicity in SH-SY5Y cells by regulating the SIRT1-activated PI3K/AKT pathway

Bin Liu and Yuan Wei

Department of Anesthesiology, Wujin Hospital Affiliated to Jiangsu

University (Wujin School of Clinical Medicine, Xuzhou Medical University), Changzhou, Jiangsu, PR China

Summary. Urolithin A (UroA) is well-recognized for its anti-oxidative, anti-inflammatory, and immuno-modulatory potentials and has been proven to have neuroprotective effects. Nevertheless, the potential of UroA on bupivacaine (BUP)-induced neurotoxicity has never been reported. Using SH-SY5Y cells to establish a cell model, it was revealed that BUP stimulated cell viability reduction, LDH release increase, and suppression of SIRT1-activated PI3K/AKT signaling in SH-SY5Y cells, whereas UroA treatment caused an effective abrogation of the effects of BUP. Besides, SIRT1 overexpression caused an enhancement in the activity of PI3K/AKT signaling in BUP and UroA co-treated cells, indicating that SIRT1 mediated the activity of PI3K/AKT signaling. Moreover, UroA inhibited BUP-induced apoptosis, oxidative stress, and inflammatory responses in SH-SY5Y cells. However, the effects of UroA on BUP-induced neurotoxicity were all abated by inhibiting SIRT1 or PI3K/AKT signaling through EX527 or LY294002. In conclusion, UroA protected SH-SY5Y cells against BUP-induced injuries through PI3K/AKT signaling in a SIRT1-dependent manner.

Key words: Urolithin A, SIRT1, PI3K/AKT, Bupivacaine, Neurotoxicity

Introduction

Local anesthetics are commonly used clinically to alleviate surgical pain, post-operative pain, or chronic pain (Deng et al., 2022; Lu et al., 2022). Bupivacaine (BUP), an amide-type local anesthetic, has been

extensively used for nerve blockade, and epidural or spinal anesthesia in clinical patients to provide excellent sensory anesthesia (Mirkheshti et al., 2020). However, exposure to BUP has been reported to induce neurotoxicity (Beiranvand et al., 2016). To date, the mechanism underlying the toxicity of BUP has remained largely unclarified. Therefore, it is essential to deepen our understanding of BUP-induced neurotoxicity.

Urolithin A (UroA) is a type of urolithin naturally yielded by the intestinal microbiota from ellagitannins and ellagic acid (Cortés-Martín et al., 2019). Urolithins are reported to have anti-oxidative, anti-inflammatory, and immunomodulatory potentials, especially UroA (Aya et al., 2021; D'Amico et al., 2021). More importantly, UroA has been revealed to exert neuroprotective effects in human diseases. For example, UroA acted as a neuroprotectant by ameliorating oxidative stress in Neuro-2a cells (Cásedas et al., 2020). UroA activated autophagy to protect against ischemic neuronal injury by repressing ER stress (Ahsan et al., 2019). UroA protected neurons from cognitive impairment via anti-inflammatory signaling in a mouse model of Alzheimer's disease (Gong et al., 2019). Particularly, neuroprotective effects of urolithins against oxidative stress-induced cytotoxicity were reported in SH-SY5Y cells (González-Sarrías et al., 2017). However, the role of UroA has never been investigated in BUP-induced neurotoxicity.

The PI3K/AKT pathway affects multiple intracellular activities to directly or indirectly influence cell apoptosis (Duronio, 2008). The modulation of PI3K/AKT signaling on cell apoptosis in human diseases has been widely reported. For instance, sciadopitysin activated PI3K/AKT/GSK-3β signaling to protect cardiomyocytes from oxidative stress and apoptosis in high glucose conditions (Zhang et al., 2021). ANXA2P2 suppressed glioblastoma progression by inhibiting the PI3K/AKT pathway (Ni et al., 2021). BUP stimulated apoptosis and ferroptosis through the inhibition of PI3K/Akt signaling in bladder cancer (Hao et al., 2022).

Corresponding Author: Yuan Wei, Department of Anesthesiology, Wujin Hospital Affiliated to Jiangsu University (Wujin School of Clinical Medicine, Xuzhou Medical University), No. 2 Yongning North Road, Hongmei Street, Tianning District, Changzhou, Jiangsu, 213000, PR China. e-mail: yuan_wei123@126.com

It is still unknown whether UroA mediates SH-SY5Y cell apoptosis induced by BUP via the PI3K/AKT pathway.

This work hypothesized that UroA exerted neuroprotective effects on BUP-induced neural injuries by enhancing the activity of the PI3K/AKT pathway. It was revealed that UroA treatment significantly attenuated BUP-induced impairment of cell viability, oxidative stress, and inflammatory responses in SH-SY5Y cells.

Materials and methods

Cell culture and treatment

The neuroblastoma cell line SH-SY5Y (ATCC) was cultured in DMEM (ThermoFisher Scientific, USA) supplemented with 10% FBS and 100 U/mL penicillin-streptomycin in a humidified incubator (5% CO_2; 37°C). UroA (MedChemExpress LLC, purity >98%) was dissolved in DMSO (Sigma-Aldrich) to prepare a 100-mM stock as previously described (El-Wetidy et al., 2021). For subsequent experiments, SH-SY5Y cells were treated with 50 μM UroA, 1.5 mM BUP (Sigma-Aldrich, USA), PI3K/AKT inhibitor (LY294002, 10 μM, Sigma-Aldrich), and/or SIRT1 inhibitor (EX527, 1 μM, Selleck) for 24h.

Plasmid and lentivirus infection

For SIRT1 overexpression, the nucleotide sequence of SIRT1 [NM_012238.5] was cloned into a pLV expression Vector (VectorBuilder, Chicago, USA), and eGFP was cloned into a pLV vector as a control. Lentiviruses encapsulating the SIRT1 expression vector or the control were produced in HEK-293FT cells and used to infect SH-SY5Y cells. The infected cells were selected using puromycin (2 μg/mL for 2 days) for further experiments.

CCK-8 assay

The viability of SH-SY5Y cells was assessed using the CCK-8 assay. Cells were treated with increasing concentrations of UroA (0, 25, 50, or 100 μM), BUP (0, 0.5, 1.0, or 1.5 mM), 1.5 mM BUP + UroA (0, 25, 50, or 100 μM) for 24h, or with 100 μM UroA and/or 1.5 mM BUP for 0, 24, 48, and 72h.

TUNEL

Apoptosis of treated SH-SY5Y cells was evaluated using a fluorometric TUNEL assay kit (Promega, USA).

Flow cytometry

To evaluate cell apoptosis, SH-SY5Y cells subjected to the specified treatments were collected, PBS-washed twice, and then suspended in 200 μL of 1×Annexin V-binding buffer. Subsequently, cells underwent dual staining with Annexin V-fluorescein isothiocyanate (FITC) and propidium iodide (PI) using the Dead Cell Apoptosis kit from ThermoFisher Scientific, Inc. After incubation for 15 minutes in the dark, apoptotic cells were quantified using a FCM flow cytometer equipped with FlowJo software (BD Bioscience, San Jose, CA, USA).

Immunofluorescence staining

After the designated treatments, the intracellular level of reactive oxygen species (ROS) was gauged employing the redox-sensitive fluorescent probe, 2',7'-dichlorofluorescein diacetate (DCFH-DA) obtained from Sigma-Aldrich. Briefly, SH-SY5Y cells were seeded into 96-well cell culture plates (1×10^4 cells/well) and exposed to 10 μM DCFH-DA for 30 minutes in the absence of light at 37°C. Subsequently, the fluorescence emitted by the oxidized probe was measured at an excitation/emission wavelength of 485/530 nm using a microplate reader from BioTek Instruments.

Measurement of biochemicals

The supernatants of treated SH-SY5Y cells were collected to determine the lactate dehydrogenase (LDH) level using the LDH cytotoxicity assay kit (G-Biosciences, USA). The levels of catalase (CAT), superoxide dismutase (SOD), glutathione peroxidase (GSH-Px), and malondialdehyde (MDA) were detected via specific commercial kits including the Catalase assay kit (Visible light, A007-1-1), Superoxide Dismutase assay kit (WST-1 method, A001-3-2), Glutathione Peroxidase assay kit (Colorimetric method, A005-1-2), and Malondialdehyde assay kit (TBA method, A003-1-2) (Nanjing Jiancheng Bioengineering Institute, China) according to the manufacturer's instructions.

ELISA

The levels of pro-inflammatory cytokines (IL-6, IL-1β, and TNF-α), were detected using commercial ELISA kits (R&D Systems, USA).

Western blot

Following previous steps (Zhao and Wang, 2020), western blot was conducted using the primary antibodies sourced from Abcam, including anti-SIRT1 (ab110304), anti-PI3K (ab191606), anti-p-PI3K (ab182651), anti-AKT (ab8805), anti-p-AKT (ab38449), antiPARP1 (ab32064), cleaved caspase-3 (ab32042), LC3B (ab192890), P62 (ab192890), and β-actin (ab8226).

Statistical analysis

Statistics were subjected to analysis by SPSS16.0 software (SPSS Inc.). Data are expressed as mean ±

standard deviation of three independent experiments. Statistical comparison was conducted using one-way ANOVA. *P*<0.05 was regarded as statistically significant.

Results

UroA attenuated BUP-induced neurotoxicity

Firstly, the cytotoxicity of UroA and BUP in SH-SY5Y cells was evaluated. The CCK-8 assay showed that treatment with UroA at increasing concentrations (0,

25, 50, or 100 μM) or 100 μM at increasing times (0, 24, 48, and 72h) caused no significant change in the viability of SH-SY5Y cells in comparison with untreated cells (Fig. 1A,B). Nevertheless, the viability of SH-SY5Y cells was inhibited by BUP in a dose- and time-dependent manner (Fig. 1C,D). Intriguingly, cells challenged with 1.5 mM BUP exhibited increased viability following UroA treatment (Fig. 1E,F). Therefore, UroA may have ameliorative potential on BUP-induced cytotoxicity in SH-SY5Y cells.

UroA activated PI3K/AKT signaling in BUP-stimulated SH-SY5Y cells through the upregulation of SIRT1

To determine the molecular mechanism of UroA, the expression of SIRT1 and PI3K/AKT signaling proteins were assessed in SH-SY5Y cells after the designated treatments. It was discovered that the levels of SIRT1, phosphorylated PI3K (p-PI3K), and AKT (p-AKT) were remarkably suppressed by BUP treatment, the introduction of UroA ameliorated the suppression triggered by BUP (Fig. 2A). Subsequently, SIRT1 inhibitor (EX527) or PI3K/AKT-specific inhibitor (LY294002) was used to treat BUP-challenged cells after UroA treatment. Western blot showed that EX527 noticeably reduced the levels of SIRT1, p-PI3K, and p-AKT while LY294002 only inhibited the expression of p-PI3K and p-AKT compared with that in the UroA treatment group (Fig. 2A). Moreover, LY294002 overturned the upregulation of p-PI3K and p-AKT caused by SIRT1 overexpression (Fig. 2B). Taken together, UroA upregulated SIRT1 to activate PI3K/AKT signaling in BUP-challenged SH-SY5Y cells.

UroA revived BUP-stimulated suppression of cell viability via SIRT1/PI3K/AKT signaling

After understanding the molecular mechanism of UroA in BUP-challenged SH-SY5Y cells, we further investigated the participation of the SIRT1 and PI3K/AKT pathways in the possible therapeutic effects of UroA on BUP-induced neurotoxicity. Fig. 3A illustrated that the impact of UroA on cell viability was insignificant while BUP induced a marked decrease in the viability of SH-SY5Y cells. The suppressed cell viability induced by BUP treatment was rescued by UroA but the introduction of EX527 or LY294002 annulled the effect of UroA. Consistently, UroA relieved the upregulation of LDH release in SH-SY5Y cells caused by BUP treatment, which, however, was re-elevated when SIRT1 activity or PI3K/AKT signaling was inhibited (Fig. 3B). These results showed that UroA ameliorated BUP-triggered SH-SY5Y cell injury through SIRT1/PI3K/AKT signaling.

UroA alleviated BUP-induced apoptosis and autophagy through the SIRT1-activated PI3K/AKT pathway
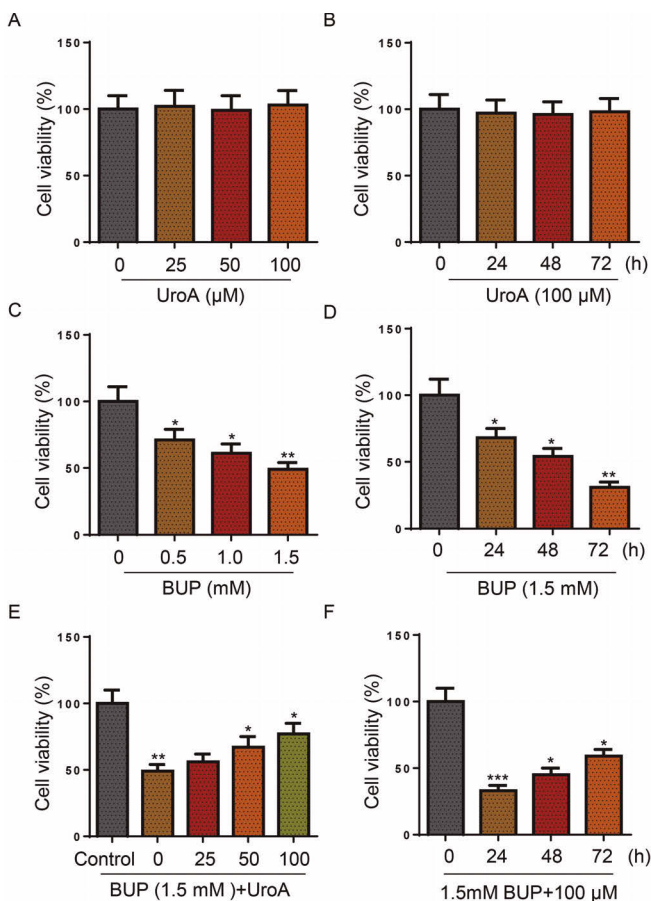
Subsequently, TUNEL and flow cytometry assays

Fig. 1. Evaluation of the cytotoxicity of UroA or BUP in SH-SY5Y cells. **A.** Cell viability was detected using the CCK-8 assay after treatment with UroA (0, 25, 50, or 100 μM) for 24h. **B.** The viability of SH-SY5Y cells treated with 100 μM UroA for 0, 24, 48, and 72h. **C.** Viability of SH-SY5Y cells treated with BUP (0, 0.5, 1.0, and 1.5 mM) for 24h. **D.** Viability of SH-SY5Y cells treated with 1.5 mM BUP for 0, 24, 48, and 72h. **E.** Viability of SH-SY5Y cells treated with 1.5 mM BUP + UroA (0, 25, 50, or 100 μM) for 24h. **F.** Viability of SH-SY5Y cells treated with 1.5 mM BUP + 100 μM UroA for 0, 24, 48, and 72h. *P<0.05; **P<0.01.

were conducted to evaluate the apoptosis of treated SH-SY5Y cells. It was revealed that the change in apoptosis rate in the UroA group was not significant compared with the control group, BUP treatment caused a drastic increase in cell apoptosis. Moreover, EX527 or LY294002 abated the suppressive effect of UroA on BUP-induced cell apoptosis (Fig. 4A,B). In agreement, western blot detected that UroA treatment did not affect the expression of cleaved PARP and cleaved caspase-3 but attenuated the upregulation of those two proteins caused by BUP treatment. Meanwhile, inhibition of SIRT1 activity or the PI3K/AKT pathway rescued UroA-stimulated suppression of cleaved PARP and cleaved caspase-3 protein levels (Fig. 4C). The changes in the expression of autophagy-related proteins (LC3 and p62) indicated UroA suppressed BUP-induced autophagy activity, the effect of UroA was abrogated by either EX527 or LY294002 (Fig. 4D). Therefore, UroA suppressed BUP-triggered apoptosis and autophagy in SH-SY5Y cells via the SIRT1-mediated PI3K/AKT pathway.

UroA activated the SIRT1/PI3K/AKT pathway to inhibit BUP-induced oxidative stress

It was found that UroA had no effect on ROS production but could suppress the BUP-stimulated ROS in SH-SY5Y cells while the introduction of SIRT1 or PI3K/AKT inhibitors re-elevated ROS the production suppressed by UroA (Fig. 5A). In addition, BUP-stimulated cells exhibited increased MDA content and diminished activities of GSH-Px, SOD, and CAT, which were effectively abrogated by UroA participation. UroA barely affected these indexes when cells were not treated with BUP. Moreover, the inhibitory effect of UroA on MDA content and the promotive effect of UroA on GSH-Px, SOD, and CAT activities in BUP-challenged cells was reversed by inhibiting SIRT1 or blocking the PI3K/AKT pathway (Fig. 5B-E). All in all, UroA mediated SIRT1 activity and the PI3K/AKT pathway to alleviate BUP-induced oxidative stress in SH-SY5Y cells.

UroA alleviated BUP-induced inflammatory response via the SIRT1/PI3K/AKT pathway

Inflammation is an important index of neural injury (Tseng et al., 2021). The effect of UroA on inflammatory responses in BUP-treated cells was investigated by assessing the levels of proinflammatory cytokines (IL-6, IL-1β, and TNF-α) using an ELISA assay. The levels of these cytokines were dramatically elevated in BUP-treated cells but not in UroA-treated cells. Additionally, UroA ameliorated the inflammatory responses triggered
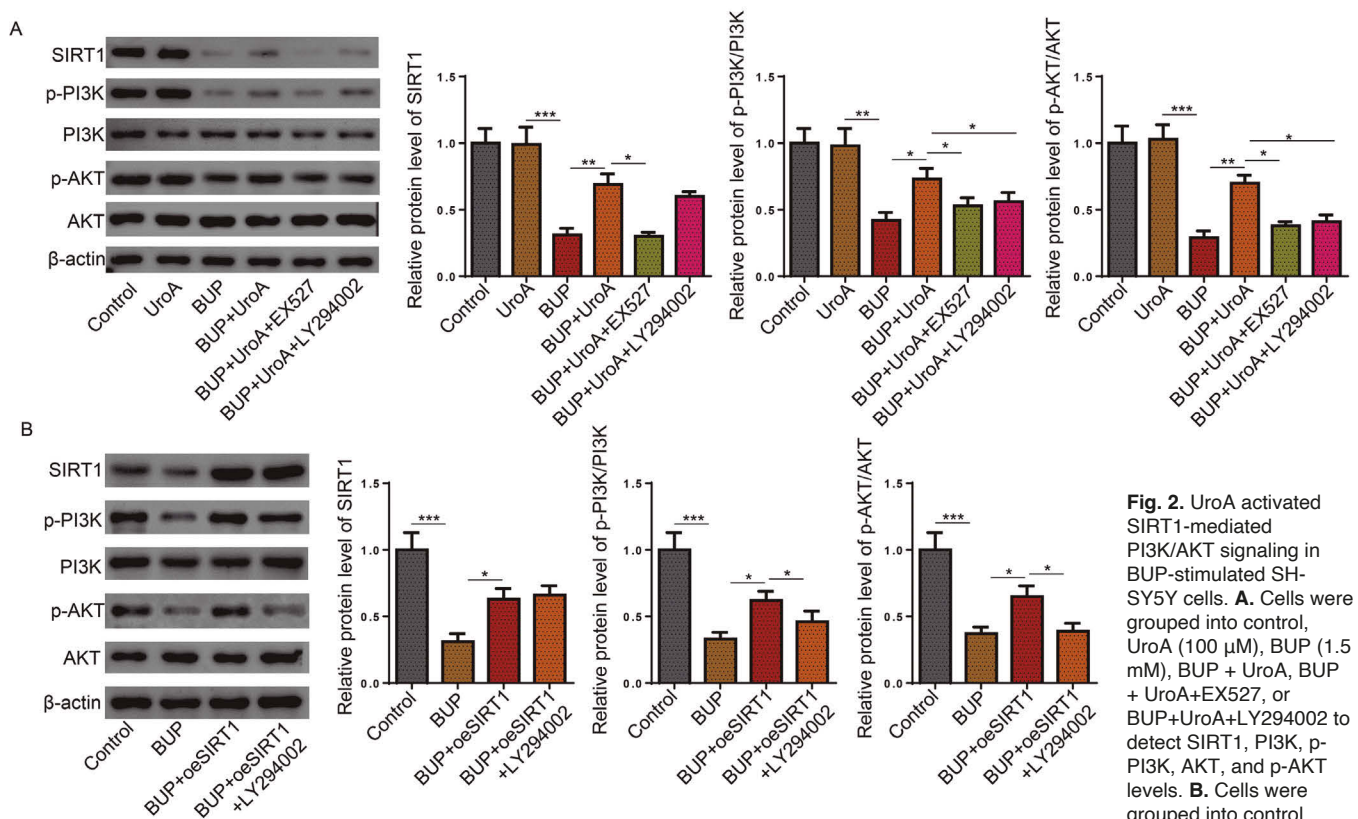

Fig. 2. UroA activated SIRT1-mediated PI3K/AKT signaling in BUP-stimulated SH-SY5Y cells. **A.** Cells were grouped into control, UroA (100 μM), BUP (1.5 mM), BUP + UroA, BUP + UroA+EX527, or BUP+UroA+LY294002 to detect SIRT1, PI3K, p-PI3K, AKT, and p-AKT levels. **B.** Cells were grouped into control, BUP (1.5 mM), BUP + oeSIRT1, or BUP + oeSIRT1+LY294002 to detect the levels of PI3K, p-PI3K, AKT, and p-AKT. *$P<0.05$; **$P<0.01$; ***$P<0.001$.
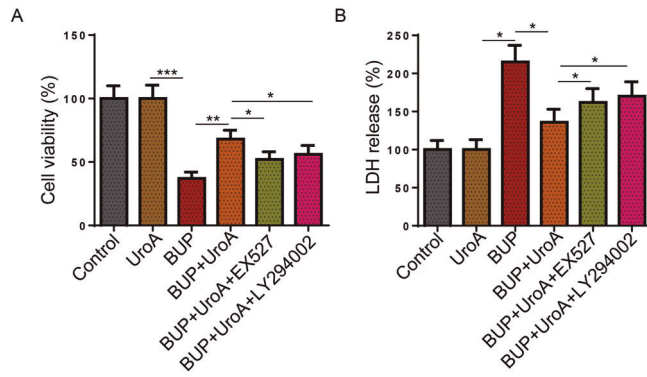
Fig. 3. Effect of UroA on the viability of BUP-challenged SH-SY5Y cells. Cells were divided into Control, UroA, BUP, BUP + UroA, BUP + UroA + EX527, and BUP + UroA + LY294002. **A.** Cell viability was detected using the CCK-8 assay kit. **B.** LDH release was assessed using the LDH cytotoxicity assay kit. *$P<0.05$; **$P<0.01$; ***$P<0.001$.
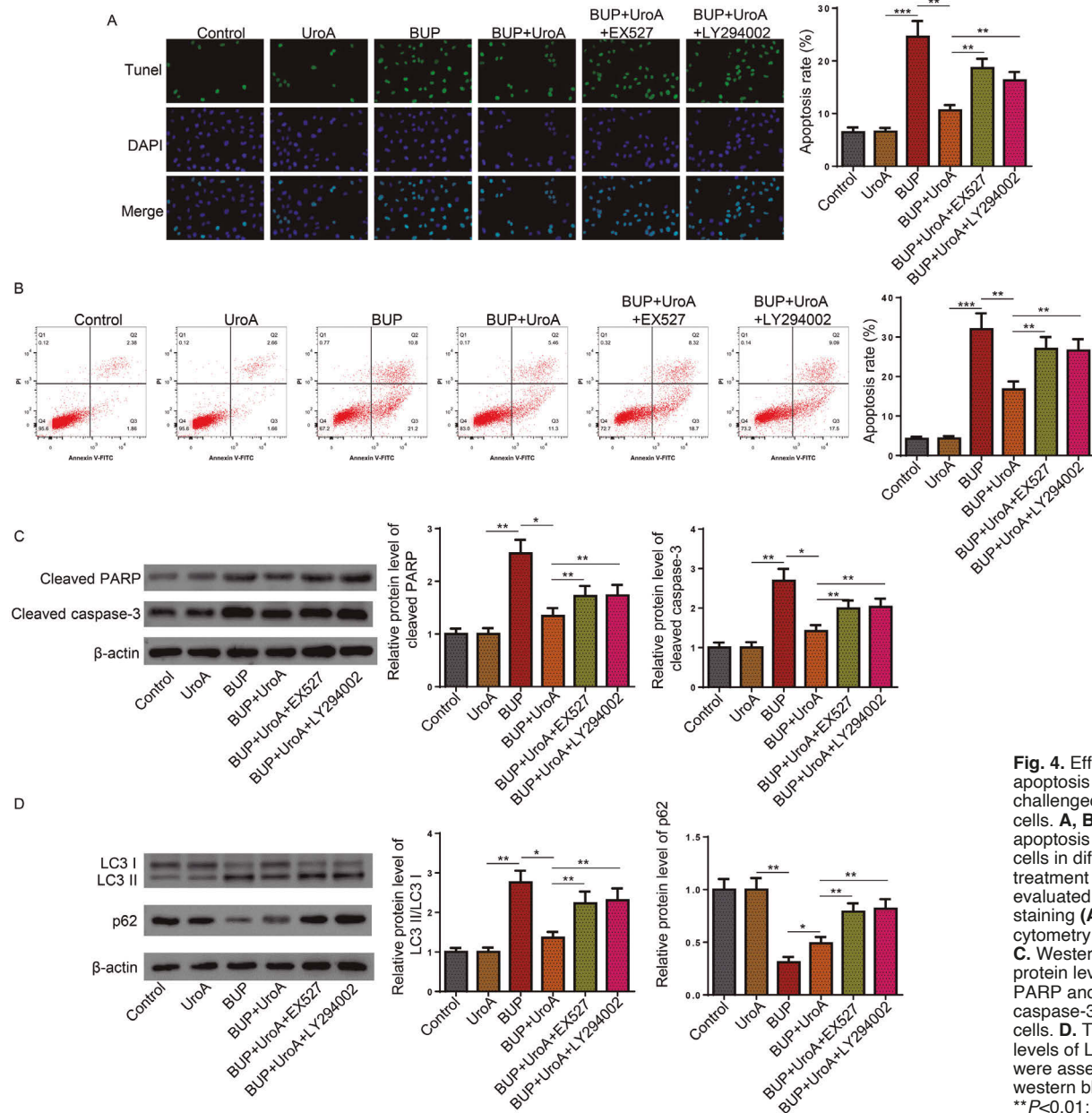

Fig. 4. Effect of UroA on apoptosis of BUP-challenged SH-SY5Y cells. **A, B.** The apoptosis of SH-SY5Y cells in different treatment groups was evaluated using TUNEL staining **(A)** and flow cytometry **(B)**. **C.** Western blot detected protein levels of cleaved PARP and cleaved caspase-3 in treated cells. **D.** The protein levels of LC3 and P62 were assessed using western blot. *$P<0.05$; **$P<0.01$; ***$P<0.001$.

by BUP, which were further annulled when SIRT1 expression was silenced or the PI3K/AKT pathway was blocked (Fig. 6A-C), suggesting that UroA suppressed the expression of IL-6, IL-1β, and TNF-α in BUP-challenged SH-SY5Y cells through the SIRT1-mediated PI3K/AKT pathway.

Discussion

BUP, levobupivacaine, and ropivacaine are the most used amide-based local anesthetics (Kucharova et al., 2019). Since the introduction of BUP into clinical practice, an increase in severe cardiovascular and central nervous system toxicity has been reported (Waldinger et al., 2020). Accumulating studies have been dedicated to

the discovery of methods and underlying mechanisms involved in ameliorating BUP-induced neurotoxicity. For instance, melatonin alleviated BUP-induced spinal neurotoxicity via the inhibition of the NLRP3 inflammasome in rats (Lai et al., 2022). Increased TRPM7 activities exacerbated BUP-stimulated neurotoxicity in high glucose pre-conditioned SH-SY5Y cells (Dai et al., 2021). Inhibition of CaMK2α-MCU signaling mitigated BUP-induced neurotoxic injuries by suppressing mitochondrial oxidative stress (Liu et al., 2020). Herein, a BUP-induced neurotoxic cell model in SH-SY5Y cells was established to study the neuroprotective potential and mechanism of UroA. It was revealed that UroA ameliorated the viability impairment and LDH release of SH-SY5Y cells induced
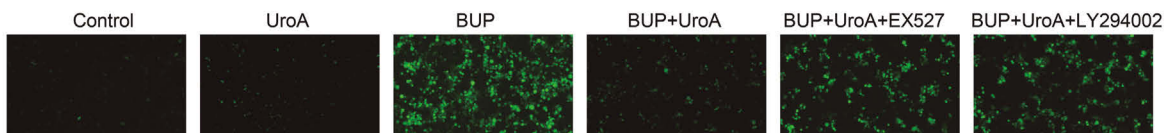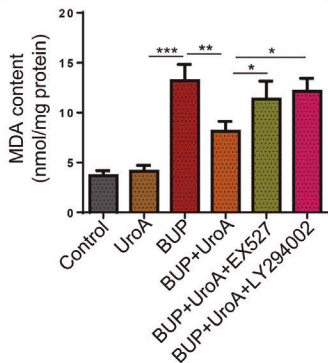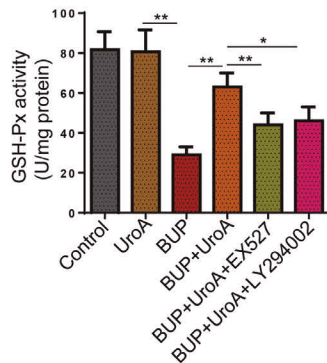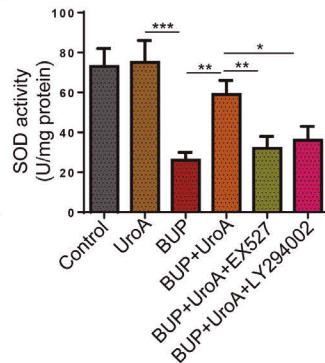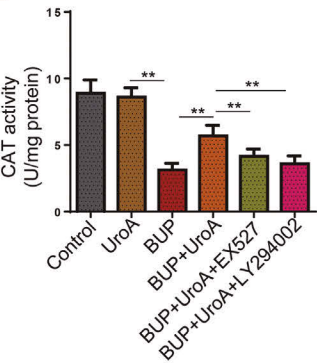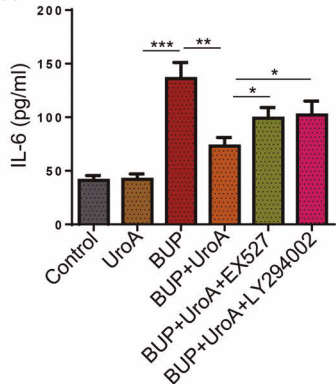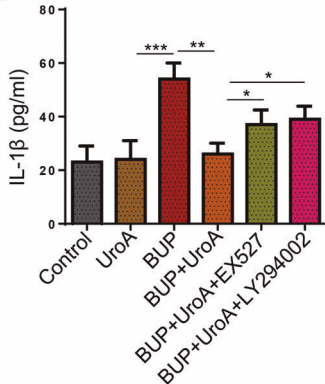

Fig. 5. Effect of UroA on the oxidative stress of BUP-challenged SH-SY5Y cells. **A.** The intracellular ROS level was reflected using IF staining. **B-E.** Detection of oxidative indexes: MDA content **(B)**, GSH-Px **(C)**, SOD **(D)**, and CAT **(E)** in SH-SY5Y cells. *$P<0.05$; **$P<0.01$; ***$P<0.001$.
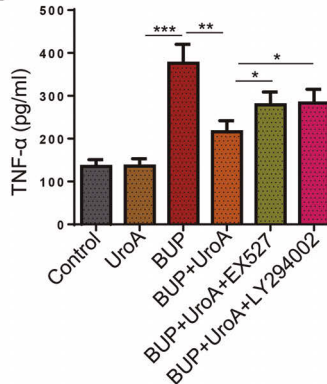

Fig. 6. Effect of UroA on the inflammatory responses of BUP-challenged SH-SY5Y cells. **A-C.** Detection of proinflammatory cytokines: IL-6 **(A)**, IL-1β **(B)**, and TNF-α **(C)**. *$P<0.05$; **$P<0.01$; ***$P<0.001$.

by BUP.

Evidence showed that UroA could promote the activity of SIRT1 in many cases. For instance, UroA alleviated streptozotocin-induced diabetic cardiomyopathy through the activation of SIRT1 in rats (Albasher et al., 2022). UroA induced SIRT1 expression to protect dopaminergic neurons in cell and mouse models of Parkinson's disease (Liu et al., 2022; Qiu et al., 2022). UroA alleviates the senescence of nucleus pulposus-derived mesenchymal stem cells triggered by oxidative stress through the activation of the SIRT1/PGC-1α pathway (Shi et al., 2021). In addition, SIRT1 has been frequently reported to mediate the activity of PI3K/AKT signaling (Chai et al., 2017; Li and Wang, 2017; Liu et al., 2019). Moreover, PI3K/AKT signaling plays an active role in the neuroprotective effects of various chemicals or natural compounds. For example, capillarisin ameliorated BUP-induced injuries in SH-SY5Y cells by activating PI3K/AKT (Zhao and Wang, 2020). Neuregulin-1 rescued primary cortical neurons from apoptosis by the stimulation of PI3K/AKT signaling in Alzheimer's Disease (Baik et al., 2016). *Coeloglossum viride var. bracteatum* extract restored the FGF2-PI3K/Akt pathway to alleviate staurosporine-induced neurotoxicity (Cai et al., 2021). This work demonstrated that UroA upregulated SIRT1 to activate PI3K/AKT signaling in BUP-challenged SH-SY5Y cells.

Furthermore, the influence of UroA treatment on BUP-induced injuries in SH-SY5Y cells was evaluated in terms of cell viability, cell apoptosis, oxidative stress, and inflammatory responses, which are pivotal indexes for BUP-induced neurotoxicity (Chen et al., 2018; Wang et al., 2021; Zhang et al., 2019). Our results demonstrated that BUP stimulated the suppression of cell viability, upregulation of LDH release, enhancement of cell apoptosis, activation of oxidative stress, and promotion of inflammatory responses in SH-SY5Y cells, whereas UroA effectively ameliorated injuries caused by BUP by triggering the activity of SIRT1/PI3K/AKT signaling.

Collectively, UroA was revealed to act as a neuroprotectant in BUP-stimulated neurotoxicity in SH-SY5Y cells by improving cell viability, inhibiting cell apoptosis, suppressing oxidative stress, and alleviating inflammatory responses. In addition, the therapeutic effects of UroA were achieved by activating PI3K/AKT signaling via SIRT1 in BUP-challenged cells. The safer profile of Urolithin A as a natural compound has given new hope for the design of new adjuvant therapeutic approaches aimed at reducing the neurotoxic effects of BUP.

References

Ahsan A., Zheng Y.R., Wu X.-L., Tang W.-D., Liu M.-R., Ma S.-J., Jiang L., Hu W.-W., Zhang X.-N. and Chen Z. (2019). Urolithin A-activated autophagy but not mitophagy protects against ischemic neuronal injury by inhibiting ER stress *in vitro* and *in vivo*. CNS Neurosci. Ther. 25, 976-986.

Albasher G., Alkahtani S. and Al-Harbi L.N. (2022). Urolithin A prevents streptozotocin-induced diabetic cardiomyopathy in rats by activating SIRT1. Saudi J. Biol. Sci. 29, 2, 1210-1220.

Aya V., Flórez A., Perez L. and Ramírez J.D. (2021). Association between physical activity and changes in intestinal microbiota composition: A systematic review. PLoS One 16, e0247039.

Baik T.K., Kim Y.J., Kang S.M., Song D.-Y., Min S.S. and Woo R.-S. (2016). Blocking the phosphatidylinositol 3-kinase pathway inhibits neuregulin-1-mediated rescue of neurotoxicity induced by Aβ1-42. J. Pharm. Pharmacol. 68, 8, 1021-1029.

Beiranvand S., Eatemadi A. and Karimi A. (2016). New updates pertaining to drug delivery of local anesthetics in particular bupivacaine using lipid nanoparticles. Nanoscale Res. Lett. 11, 307.

Cásedas G., Les F., Choya-Foces C., Hugo M. López V. (2020). The metabolite urolithin-A ameliorates oxidative stress in neuro-2a cells, becoming a potential neuroprotective Agent. Antioxidants 9, 177.

Cai Z.P., Cao C., Guo Z., Yu Y., Zhong S.-J., Pan R.-Y., Liang H., Lan R. and Qin X.-Y. (2021). *Coeloglossum viride var. bracteatum* extract attenuates staurosporine induced neurotoxicity by restoring the FGF2-PI3K/Akt signaling axis and Dnmt3. Heliyon 7, e07503.

Chai R., Fu H., Zheng Z., Liu T., Ji S. and Li G. (2017). Resveratrol inhibits proliferation and migration through SIRT1 mediated post-translational modification of PI3K/AKT signaling in hepatocellular carcinoma cells. Mol. Med. Rep. 16, 8037-8044.

Chen L., Li Q., Wang H., Chen Q., Wu Y. and Shang Y. (2018). Paeoniflorin attenuated bupivacaine-induced neurotoxicity in SH-SY5Y cells via suppression of the p38 MAPK pathway. J. Cell. Biochem. 120, 7015-7023.

Cortés-Martín A., Romo-Vaquero M., García-Mantrana I., Rodríguez-Varela A., Collado M.C., Espín J.C. Selma M.V. (2019). Urolithin metabotypes can anticipate the different restoration of the gut microbiota and anthropometric profiles during the first year postpartum. Nutrients 11, 2079.

D'Amico D., Andreux P.A., Valdés P., Singh A. Rinsch C. and Auwerx J. (2021). Impact of the natural compound urolithin A on health, disease, and aging. Trends Mol. Med. 27, 687-699.

Dai S. H., Li Y.W., Hong Q.X., Su T. and Xu S.-Y. (2021). Exaggerated activities of TRPM7 underlie bupivacaine-induced neurotoxicity in the SH-SY5Y cells preconditioned with high glucose. J. Biochem. Mol. Toxicol. 35, e22826.

Deng W., Yan Y., Zhuang P., Liu X., Tian K., Huang W. and Li C. (2022). Synthesis of nanocapsules blended polymeric hydrogel loaded with bupivacaine drug delivery system for local anesthetics and pain management. Drug Deliv. 29, 399-412.

Duronio V. (2008). The life of a cell: apoptosis regulation by the PI3K/PKB pathway. Biochem. J. 415, 333-344.

El-Wetidy M.S., Ahmad R., Rady I., Helal H., Rady M.I., Vaali-Mohammed M., Al-Khayal K., Traiki T.B. and Abdulla M.-H. (2021). Urolithin A induces cell cycle arrest and apoptosis by inhibiting Bcl-2, increasing p53-p21 proteins and reactive oxygen species production in colorectal cancer cells. Cell Stress Chaperones 26, 473-493.

Gong Z., Huang J., Xu B., Ou Z., Zhang L., Lin X., Ye X., Kong X., Long D., Sun X., He X., Xu L., Li Q. and Xuan A. (2019). Urolithin A attenuates memory impairment and neuroinflammation in APP/PS1 mice. J. Neuroinflammation 16, 62.

González-Sarrías A., Núñez-Sánchez M., Tomás-Barberán F.A. and Espín J.C. (2017). Neuroprotective effects of bioavailable polyphenol-derived metabolites against oxidative stress-induced cytotoxicity in human neuroblastoma SH-SY5Y Cells. J. Agric. Food Chem. 65, 752-758.

Hao J., Zhang W. and Huang Z. (2022). Bupivacaine modulates the apoptosis and ferroptosis in bladder cancer via phosphatidylinositol 3-kinase (PI3K)/AKT pathway. Bioengineered 13, 6794-6806.

Kucharova M., Astapenko D., Zubanova V., Koscakova M., Stetina R., Zadak Z. and Hronek M. (2019). Does neuraxial anesthesia as general anesthesia damage DNA? A pilot study in patients undergoing orthopedic traumatological surgery. Int. J. Mol. Sci. 21, 84.

Lai J., Ji J.-M., Chen M.-Y., Luo Y.-P., Yu Y., Zhou G., Wei L.-L., Huang L.-S. and Liu J.-C. (2022). Melatonin ameliorates bupivacaine-induced spinal neurotoxicity in rats by suppressing neuronal NLRP3 inflammasome activation. Neurosci. Lett. 772, 136472.

Li H. and Wang R. (2017). Blocking SIRT1 inhibits cell proliferation and promotes aging through the PI3K/AKT pathway. Life Sci. 190, 84-90.

Liu L., Zhu X., Zhao T., Yu Y., Xue Y. and Zou H. (2019). Sirt1 ameliorates monosodium urate crystal-induced inflammation by altering macrophage polarization via the PI3K/Akt/STAT6 pathway. Rheumatology 58, 1674-1683.

Liu Z., Zhao W., Yuan P., Zhu P., Fan K., Xia Z. and Xu S. (2020). The mechanism of CaMK2α-MCU-mitochondrial oxidative stress in bupivacaine-induced neurotoxicity. Free Rad. Biol. Med. 152, 363-374.

Liu J., Jiang J., Qiu J., Wang L., Zhuo J., Wang B., Sun D., Yu S. and Lou H. (2022). Urolithin A protects dopaminergic neurons in experimental models of Parkinson's disease by promoting mitochondrial biogenesis through the SIRT1/PGC-1α signaling pathway. Food Funct. 13, 375-385.

Lu K., Zhao L., Zhang Y., Yang F., Zhang H., Wang J., Li B., Ji G., Yu J. and Ma H. (2022). Bupivacaine reduces GlyT1 expression by potentiating the p-AMPKα/BDNF signalling pathway in spinal astrocytes of rats. Sci. Rep. 12, 1378.

Mirkheshti A., Shakeri A., Memary E., Beniasadi M., Zaringhalam J., Tajbakhsh A., Mirzaei M. and Lak E. (2020). Maternal sciatic nerve administered bupivacaine induces hippocampal cell apoptosis in offspring. BMC Anesthesiol. 20, 228.

Ni H., Zhi R., Zuo J., Liu W., Xie P. and Zhi Z. (2021). Pseudogene ANXA2P2 knockdown shows tumor-suppressive function by inhibition of the PI3K/PKB pathway in glioblastoma cells. J. Biochem. Mol. Toxicol. 35, e22824.

Qiu J., Chen Y., Zhuo J., Zhang L., Liu J., Wang B., Sun D., Yu S. and Lou H. (2022). Urolithin A promotes mitophagy and suppresses NLRP3 inflammasome activation in lipopolysaccharide-induced BV2 microglial cells and MPTP-induced Parkinson's disease model. Neuropharmacology 207, 108963.

Shi P.Z., Wang J.W., Wang P.C., Han B., Lu X.-H., Ren Y.-X., Feng X.-M., Cheng X.-F. and Zhang L. (2021). Urolithin a alleviates oxidative stress-induced senescence in nucleus pulposus-derived mesenchymal stem cells through SIRT1/PGC-1α pathway. World J. Stem Cells 13, 1928-1946.

Tseng C.T., Gaulding S.J., Dancel C.L.E. and Thorm C.A. (2021). Local activation of α2 adrenergic receptors is required for vagus nerve stimulation induced motor cortical plasticity. Sci. Rep. 11, 21645.

Waldinger R., Weinberg G. and Gitman M. (2020). Local anesthetic toxicity in the geriatric population. Drugs Aging 37, 1-9.

Wang T., Zheng L., and Zhang W. (2021). Hesperidin alleviates bupivacaine anesthesia-induced neurotoxicity in SH-SY5Y cells by regulating apoptosis and oxidative damage. J. Biochem. Mol. Toxicol. 35, e22787.

Zhang H., Wang W. and Du Q. (2019). Andrographolide attenuates bupivacaine-induced cytotoxicity in SH-SY5Y cells through preserving Akt/mTOR activity. Drug Des. Devel. Ther. 13, 1659-1666.

Zhang C., Yu H., Yang H., and Liu B. (2021). Activation of PI3K/PKB/GSK-3β signaling by sciadopitysin protects cardiomyocytes against high glucose-induced oxidative stress and apoptosis. J. Biochem. Mol. Toxicol. 35, e22887.

Zhao T. and Wang Q. (2020). Capillarisin protects SH-SY5Y cells against bupivacaine-induced apoptosis via ROS-mediated PI3K/PKB pathway. Life Sci. 259, 118279.